JACS
JOURNAL OF THE AMERICAN CHEMICAL SOCIETY
Article
pubs.acs.org/JACS

Iridium-Mediated Regioselective B−H/C−H Activation of Carborane Cage: A Facile Synthetic Route to Metallacycles with a Carborane Backbone

Zi-Jian Yao,[†] Wei-Bin Yu,[†] Yue-Jian Lin,[†] Sheng-Li Huang,[†] Zhen-Hua Li,[†] and Guo-Xin Jin*[,†,‡]

[†]Shanghai Key Laboratory of Molecular Catalysis and Innovative Material, Department of Chemistry, Fudan University, Shanghai 200433, P. R. China

[‡]State Key Laboratory of Organometallic Chemistry, Shanghai Institute of Organic Chemistry, Chinese Academy of Science, Shanghai 200032, P. R. China

Supporting Information

ABSTRACT: One-pot reactions of carborane carboxylic acids (L), $[Cp^*IrCl_2]_2$, and silver salt are reported, which lead to regioselective B−H or C−H bond activation at ambient temperature in good yields. This process is demonstrated for three carborane (*o*-, *m*-, *p*-) dicarboxylates, and metal-mediated B−H functionalization of a *p*-carborane derivative is accomplished for the first time. Two metal-induced self-assembly routes to tetra-nuclear metallacycles **3** and **5** were performed through B(4, 7)/H and B(2, 10)/H activation, respectively, and the two metallacycles were found to be stable and to exist in solution as discrete complexes. Different activation modes in the carborane cage were ascribed to the characteristic structure of the products and the electronic density differences. The analogous reaction of *o*-carborane monocarboxylate with the same metal precursor gave the C−H activation complex **6**, indicating that the B−H bond is more stable than the C−H bond in this carborane cage. The selective activation was confirmed by DFT calculation results. In this study, a facile and efficient synthetic route has been developed through specific B−H bond activation to construct carborane-based metallacycles that are unavailable by conventional methods.

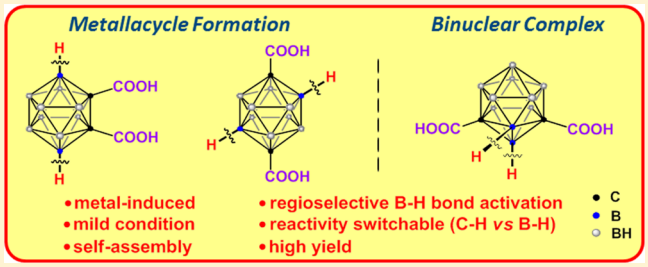

1. INTRODUCTION

Transition metal−boryl complexes[1] are important intermediates in various catalytic processes,[2] including the regio-, diastereo-, and enantioselective functionalization of hydrocarbons,[3] particularly in the functionalization of alkanes due to their large abundance and low reactivity.[4] An efficient route to form such intermediates is direct activation of the B−H bond induced by transition metal complexes.[5] One of the greatest challenges associated with B−H bond activation is to achieve high selectivity for one or two B−H bonds among many related types of B−H bonds. Thus, exploration of active metal complexes and new reactions that functionalize B−H bond are being actively sought.

As one particular type of polyborane, icosahedral carboranes (*o*, *m*, *p*-$C_2B_{10}H_{12}$), containing ten B−H vertices, are largely studied because of their unique electronic and structural properties.[6] Previous results indicate that half-sandwich iridium complexes can serve as efficient reagents to induce B−H bond activation and afford the metal−boryl complexes.[7] However, the reactions almost exclusively occurred at B(3)H vertex (for *o*-carborane) and B(2)H vertex (for *m*-carborane), while the remaining vertices were inert toward such a reaction. Furthermore, to our knowledge, no B−H bond activation of *p*-carborane derivatives has been observed thus far. On the other hand, large efforts have been dedicated to metal-directed self-assembly of discrete two and three-dimensional structures (supramolecular coordination complexes, SCCs) over the past few decades due to their excellent physical and chemical properties. These types of complexes not only have the features of facile building block modularity like metal−organic frameworks (MOFs) but also could be easily characterized due to their discrete nature.[8] Excellent work in this field has been done by Stang,[9] Fujita,[10] Raymond[11] and other groups.[12] Thus, given the unusual properties of the carborane cage, design and construction of supramolecular assemblies with this cage has attracted great interest over the years, with the expectation that the supramolecular compounds will have properties in addition to those of the parent carborane molecules.[13] However, carborane derivatives in most of these cases served merely as the bridge to connect the metal fragments through the cage C-substituted groups, and the carborane cages remained intact in the reaction.

Recently, we have reported the pyrazine-Cp*Ir fragment is a useful and robust organometallic corner to prepare neutral Ir-based metallacycles.[14] The dimeric iridium(III) fragment

Received: November 14, 2013
Published: January 28, 2014

   dx.doi.org/10.1021/ja4115665 | *J. Am. Chem. Soc.* 2014, 136, 2825−2832

$[Cp^*IrCl_2]_2$(pyrazine) **2** was utilized as a building block and was linked with linear and angular aromatic dicarboxylate ligands in the reaction, which generated molecular rectangles via C−H activation under mild conditions. Inspired by these results we herein report a general and efficient process for simultaneous metallacycle formation and regiospecific B−H bond activation by using *o*, *m*, *p*-carborane dicarboxylates as building blocks, respectively (Chart 1). Regioselective B−H bond activation was implemented, induced by a dicationic Cp*Ir fragment.

Chart 1. *o*, *m*, *p*-Carborane Dicarboxylates

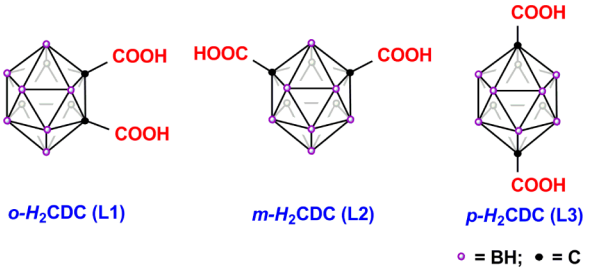

2. RESULTS AND DISCUSSION

2.1. Synthesis and Characterization of Metallacycles 3, 5, and Binuclear Complex 4. Reaction of **2**, which was prepared from the reaction of $[Cp^*IrCl_2]_2$ and pyrazine in CH_2Cl_2, with ∼4.0 equiv of AgOTf was carried out at room temperature for 6 h. Then *o*-H_2CDC **L1** and Et_3N were added into the mixture, affording red product **3** in 67% yield (Scheme 1). The signals in the ^{11}B NMR spectrum in the range of δ −3.4 to −11.7 ppm indicated that the carborane cage remained *closo*-structure. The chemical shift at δ −11.7 ppm suggested the metal−boron bond formation via cyclometalation based on our previous reports.[7] Because of the highly symmetrical structure of the complex, two singlets at δ 1.28 (Cp* groups), and 8.50 ppm (pyrazine) were observed in the ^1H NMR spectrum of **3**. Structure analysis of **3** further confirmed the construction of a metallacycle with Ir−B bond formation. Single crystals of **3** were obtained from its CH_2Cl_2/hexane solution. As shown in Figure 1, its X-ray crystal structure reveals that complex **3**

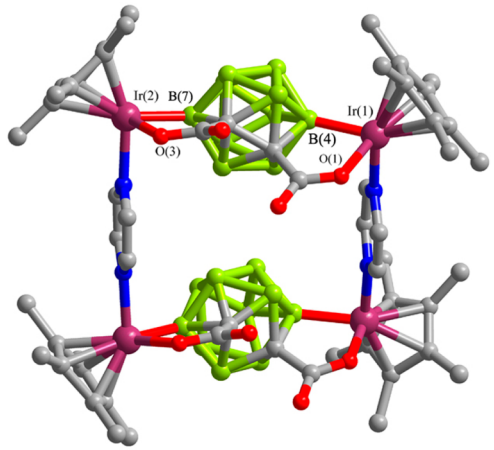

Figure 1. X-ray crystal structure of complex **3**. H atoms and solvent molecules are omitted for clarity. Plum, Ir; gray, C; red, O; blue, N; lime, B. Selected bond lengths (Å) and angles (deg): Ir(1)−B(4), 2.115(11); Ir(1)−O(1), 2.158(9); O(1)−Ir(1)−B(4), 81.1(5).

Scheme 1. Synthesis of Metallacycles 3, 5 and Binuclear Complex 4

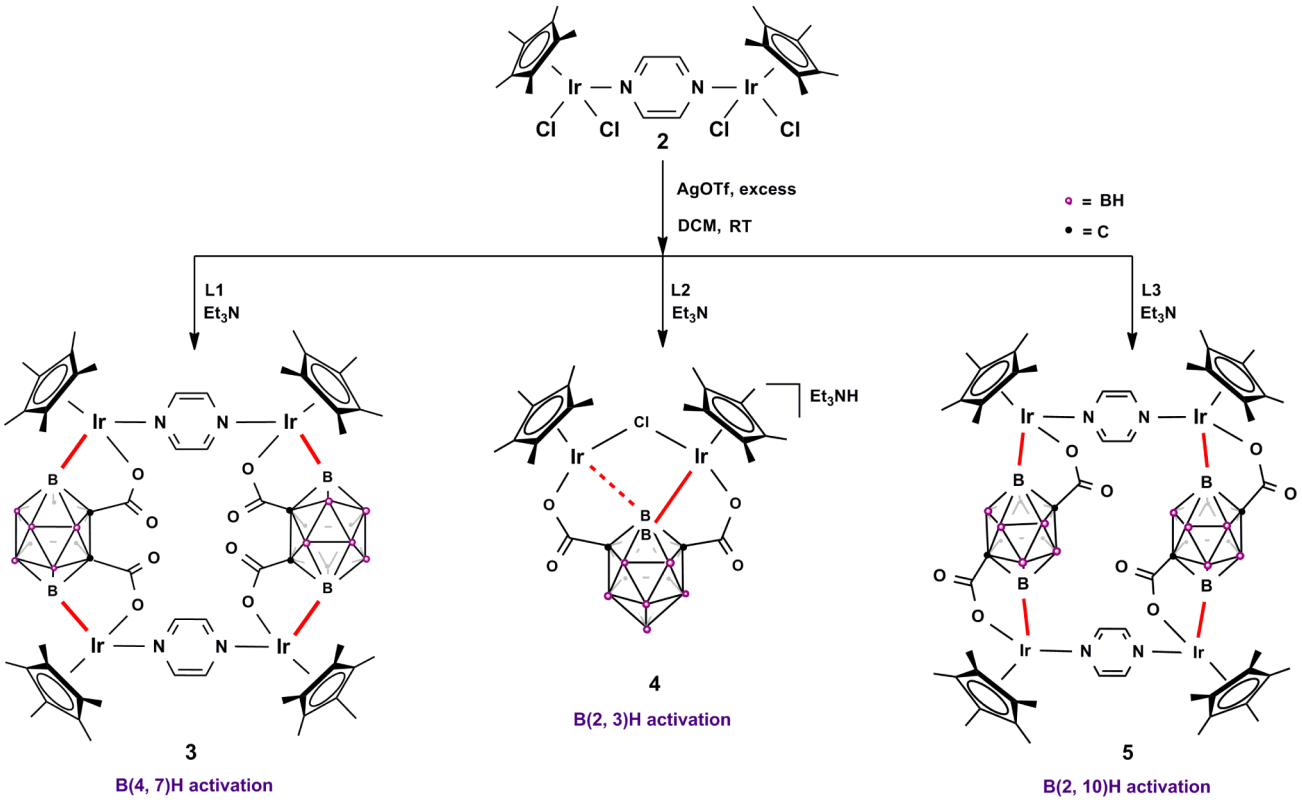

dx.doi.org/10.1021/ja4115665 | J. Am. Chem. Soc. 2014, 136, 2825−2832

possesses a distorted square structure bridged by two *o*-carborane carboxylate ligands and two pyrazine molecules with dimensions of 7.5265 Å × 6.9658 Å. The Ir−B bond length of 2.114 Å compares well with similar bonds found in other iridium−boryl complexes.[7] Interestingly, this example represents the regiospecific activation of the B(4)H and B(7)H bonds in this reaction, a pattern that is unavailable by any conventional route.[7,15] This may indicate that the B−H activation and metallacycle formation is cooperative, and that the symmetry and stability of the metallacycle prompted the particular Ir−B bond formation. The structure is stable because of the formation of four five-membered coordination cycles containing metal centers.

With the intent of exploring the scope of this synthetic approach toward different organometallic metallacycle systems and to demonstrate the regioselectivity in the B−H activation, the reactivity of *m*-H_2CDC (**L2**) and *p*-H_2CDC (**L3**) with **2** was studied under the same conditions. After evaporation of the solvent under vacuum and workup, red products of salt $[(Cp^*Ir)_2(Cl)(m\text{-}O_2C{-}C_2B_{10}H_8{-}CO_2)](Et_3NH)$ **4** and neutral $[(Cp^*Ir)_2(p\text{-}O_2C{-}C_2B_{10}H_8{-}CO_2)(pyrazine)]_2$ **5** were isolated in moderate yields (Scheme 1), respectively. Their structures were characterized by NMR spectroscopy and X-ray diffraction crystallography.

^{1}H NMR analysis of **5** indicated that its structure may be similar to that of **3**. A single peak at 1.69 ppm is attributed to protons of Cp* group, and the characteristic peak of pyrazine is clearly observed at 8.72 ppm, whose intensity ratio with respect to the Cp* protons is 2:15, suggesting originally that complex **5** is also a tetranuclear metallacycle. Molecular structures of **4** and **5** were further determined by single-crystal X-ray diffraction studies (Figure 2), which revealed unambiguously B−H activation of carborane cages. However, no construction of a iridium metallamacrocycle is noted in the formation of **4**. Notably, B−H activation at both the B(2) and B(3) positions of **4** is very rare, although B(2)H activation of carborane-based pincer complexes has been reported.[16] The loss of the pyrazine molecule in the reaction is ascribed to steric hindrance associated with the *m*-carborane carboxylate. Each iridium atom in the overall architecture of complex **4** is bound to one B atom and O atom, and they share one Cl atom. The molecular structure of **5** confirmed our structural speculation on the basis of its ^{1}H NMR spectrum. The four Cp*Ir fragments are in a distorted square environment with dimensions of 6.9546 Å (pyrazine-bridged edges) × 7.6639 Å (*p*-carborane carboxylate-bridged edges) in complex **5**. The Ir−B bond distances in **4** and **5** are 2.0756 and 2.1181 Å, respectively, which are similar to those of complex **3**. Complex **5** has been isolated as the first example of B-H activation *p*-carborane metal complex (B(2, 10) position), which has been proposed as an intermediate of alkyne and alkene borylation.

Theoretically, different isomers could be obtained in this reaction because there are different BH activation sites in the cage. However, from their crystal structure and ^{1}H NMR spectra, complexes **3** and **5** are found to be the only products obtained in the experiment because an important characteristic for the formation of isomers is the split of Cp* signals in the ^{1}H NMR. Both electronic and structural effects should be considered as possible causes for the formation of the two rectangles. A model consisting of half part of **3** was used as the model to elucidate more accurately. Each Ir atom has three activation sites in the carborane cage: B(3, 4, 5) for one Ir atom and B(6, 7, 8) for the other atom (Chart 2, left). B(3, 6)-H

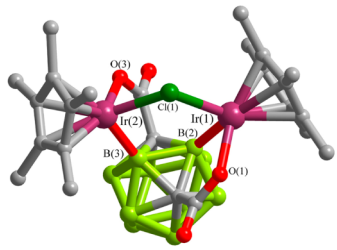

4

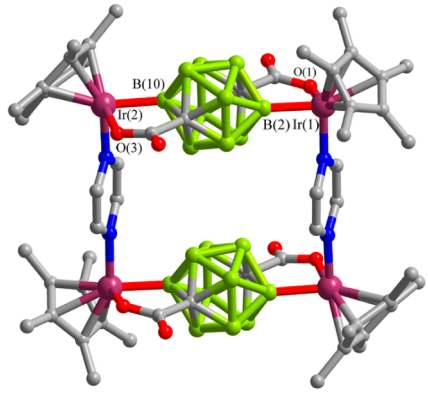

5

Figure 2. X-ray crystal structures of complexes **4** and **5**. H atoms, cations, and solvent molecules are omitted for clarity. Plum, Ir; gray, C; red, O; blue, N; lime, B; green, Cl. Selected bond lengths (Å) and angles (deg): **4**, Ir(1)−B(2), 2.100(19); Ir(1)−O(1), 2.142(14); Ir(1)−Cl(1), 2.375(5); Ir(2)−B(3), 2.08(2); Ir(2)−O(3), 2.119(14); Ir(2)−Cl(1), 2.385(5). **5**, Ir(1)−B(2), 2.12(2); Ir(1)−O(1), 2.136(16); O(1)−Ir(1)−B(2), 79.6(6).

Chart 2. Different BH Sites in L1 (left) and L3 (right)

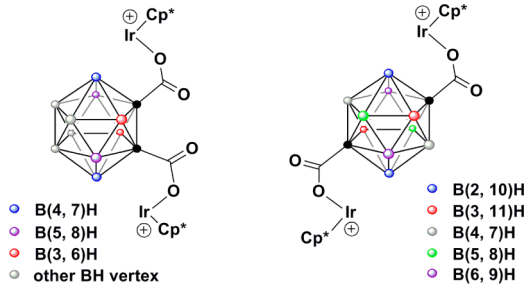

bonds are the lowest electron density positions among the 10 BH vertexes in the carborane cage,[6f,g] so activation of the B(3, 6)-H sites is not the best choice. There are four modes left now: B(4, 7), B(4, 8), B(5, 7), and B(5, 8). In reality, B(4, 7) and B(4, 8) activation modes are identical with B(5, 8) and B(5, 7) modes, respectively. The structure of obtained rectangle **3** bound through B(4, 7) is more symmetrical than that of the rectangle bound through B(4, 8) activation. For **5**, electronic density of 10 BH vertex positions is all the same. So the most symmetrical structure through B(2, 10) bond activation is preferentially obtained (the B(2, 10) activation is identical with B(3, 11), B(4, 7), B(5, 8) or B(6, 9) activation) (Chart 2, right). This is a regiospecific process, and the above reasons probably explain why **3** and **5** are the only products.

In addition to NMR characterization and elemental analysis, the carborane assemblies also were characterized via electrospray ionization mass spectrometry. ESI-MS data of complexes

dx.doi.org/10.1021/ja4115665 | J. Am. Chem. Soc. 2014, 136, 2825−2832

3 and 5 gave molecular ion peaks at m/z 1926.68 and 1926.68, respectively (Figure 3, bottom), suggesting that the rectangular

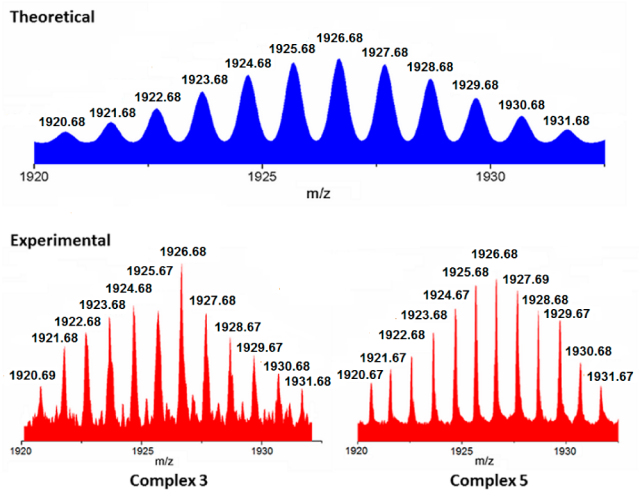

Figure 3. Theoretical (top, blue) and experimental (bottom, red) ESI-MS spectra of molecular ion peaks of complexes 3 and 5.

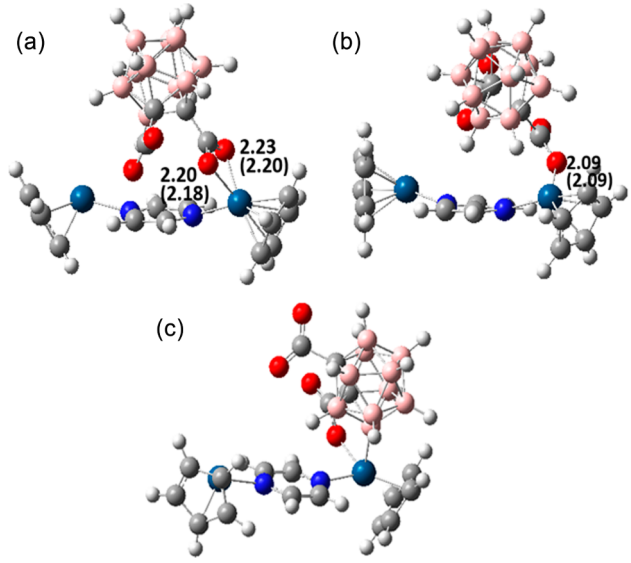

Figure 4. Geometries of the complexes between 2 and $L1^{2+}$, (a) **bd-2-L1**$^{2+}$, (b) **bd-2-L1**$^{2+}$, and (c) the deprotonated product $\mathbf{3}^{1+}$. Bond lengths (in Å) are presented, and the numbers in parentheses are those for the related Rh derivatives.

structures exist in solution as discrete complexes. The two observed peaks were isotopically resolved and are in excellent agreement with the theoretical distribution (Figure 3, top). Moreover, EI-HRMS characterization also has been done to confirm the results (1926.6781 and 1926.6779 for 3 and 5, respectively, see full mass spectra in Supporting Information, S14). In fact, metallacycles 3 and 5 were found to be very stable in air in both solution and solid state, with no detectable decomposition observed for several days in solution.

2.2. Possible Mechanism for Metallacycle 3 Formation: A DFT Study. Attempts to synthesize analogous Cp*Rh and CyRu (Cy = Cymene) complexes were not particularly successful, which indicated the great influence of the metal source. When Cp*Rh or CyRu fragments were treated with **L1-3** in the same conditions as those of the Cp*Ir fragments, no reaction was observed, indicating that neither the Rh or Ru fragments could induce B−H activation to construct metallacycles.

To gain insight into the reaction mechanism between 2 and L1, first principle calculations were carried out. The methyl groups in 2 were replaced by hydrogens to reduce computational costs. In the first step, four chloride anions of 2 were removed by AgOTf, leading to $\mathbf{2}^{4+}$. On the other hand, two protons of L1 were removed by the addition of Et_3N and $L1^{2-}$ was formed. Reaction of $\mathbf{2}^{4+}$ and $L1^{2-}$ gave a stable complex $(\mathbf{2\text{-}L1})_2^{4+}$. To reduce computational costs, we studied the properties and reactions of **2-L1**$^{2+}$ only. The dication **2-L1**$^{2+}$ has several conformers, one is a bidentate complex (**bd-2-L1**$^{2+}$) while the other is a monodentate complex (**md-2-L1**$^{2+}$) formed between the carboxyl group of $L1^{2-}$ and Ir of $\mathbf{2}^{4+}$ (Figure 4). One of the B−H bonds of **2-L1**$^{2+}$ then breaks heterolytically and loses one proton to produce the final product $\mathbf{3}^{1+}$. Our calculations indicate that the formation of **2-L1**$^{2+}$ from $\mathbf{2}^{4+}$ and $L1^{2-}$ is energetically favorable with an Gibbs free energy change (ΔG) of −66.3 kcal/mol and −53.4 kcal/mol at 298 K for the formation of **bd-2-L1**$^{2+}$ and **md-2-L1**$^{2+}$, respectively. Therefore, **bd-2-L1**$^{2+}$ is more stable than **md-2-L1**$^{2+}$ by 12.9 kcal/mol in free energy. In order to adopt a favorable conformation to produce the final product $\mathbf{3}^{1+}$ in which the carboxyl group coordinates with Ir with a monodentate configuration, **2-L1**$^{2+}$ must convert from **bd-2-L1**$^{2+}$ to **md-2-L1**$^{2+}$. The formation of the final product $\mathbf{3}^{1+}$ through a deprotonation process is energetically favorable with a ΔG of −24.4 kcal/mol. Replacing Ir with Rh, the ΔG values for the formation of **bd-2-L1**$^{2+}$ and **md-2-L1**$^{2+}$ become −80.6 kcal/mol and −64.6 kcal/mol, respectively, which indicates that **md-2-L1**$^{2+}$ is less stable than **bd-2-L1**$^{2+}$ by 15.5 kcal/mol in free energy. Since **2-L1**$^{2+}$ must adopt a monodentate configuration to produce the final product $\mathbf{3}^{1+}$, it can be concluded from the calculations that, when Ir is replaced by Rh, the production of $\mathbf{3}^{1+}$ is energetically less favorable. This is in agreement with experiment. In addition, when Ir is replaced by Rh, the deprotonation process of **2-L1**$^{2+}$ by Et_3N is also energetically less favorable with a ΔG of just −14.5 kcal/mol (−24.4 kcal/mol for Ir in comparison) for this process. Thus, from a thermodynamic point of view, the formation of 3 was more difficult after the Ir center had been replaced by Rh.

To understand why replacing Ir with Rh will not give 3, the geometries of the complexes **2-L$_1$**$^{2+}$ have been analyzed. It is shown in Figure 4 that in **bd-2-L$_1$**$^{2+}$ the two O−Ir bonds have lengths of 2.20 Å and 2.23 Å, respectively. After replacing Ir with Rh, the two O−Rh bonds become 2.18 Å and 2.20 Å, respectively. This indicates that due to the larger covalent radius (1.27 Å for Ir vs 1.25 Å for Rh) of the Ir atom, the bonds between the oxygens of carboxyl group and the metal atom are less strong in the case of the Ir species than those in the case of the Rh species. The calculations also show that the ΔG values for the formation of **bd-2-L$_1$**$^{2+}$ are −66.3 and −80.1 kcal/mol in the case of the Ir and Rh species, respectively. Therefore the complex **2-L$_1$**$^{2+}$ in the case of Ir finds it easier to adjust its conformation to adopt a favorable conformation for the later deprotonation process since **2-L$_1$**$^{2+}$ needs to break one of the two oxygen−metal bonds. This also holds true for the Ru derivative of 3 (Cp is replaced by benzene). Our calculations also show that the conversion of the bidendate conformation to monodendate conformation is more difficult in the case of the Ru analogue. On the basis of the DFT study and previous

dx.doi.org/10.1021/ja4115665 | J. Am. Chem. Soc. 2014, 136, 2825−2832

reports, a possible mechanism for the metallacycle formation was proposed (Scheme 2). The generated cationic fragment **I**

Scheme 2. Proposed Formation Mechanism of 3

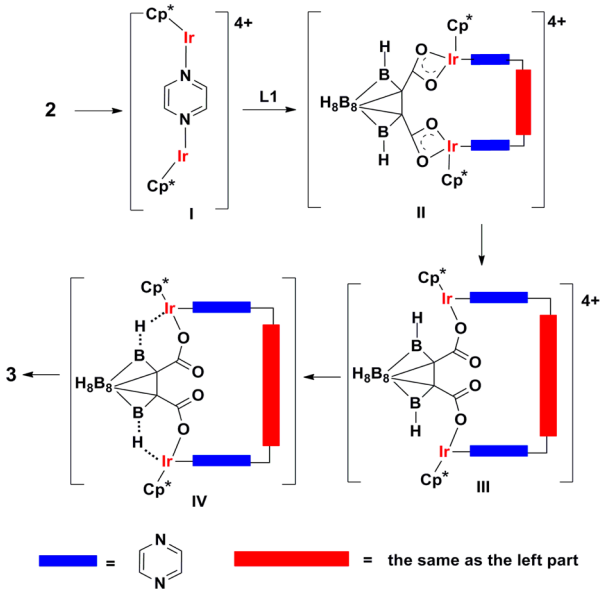

could be easily reacted with the anionic dicarboxylate ligands to give the intermediate **II** with a bidentate O, O-mode and is followed by conversion to give the monodentate intermediate **III**. A Ir···H···B three-center transition state **IV** was formed due to the electron-deficient metal center close to the electron-rich BH position.[6f] Finally, a deprotonation process occurred to give the metallacycle **3**.

2.3. Synthesis and Characterization of Binuclear Complexes 6 and 7. There are two modes of bond activation (C−H vs B−H) because two carbon atoms of the *o*-carborane cage are located adjacent to each other. Considering our previous work detailing C−H activation induced by Cp*Ir fragments,[14] we wondered which bond would be preferentially activated under identical conditions. Therefore, monosubstituted carborane carboxylate ligand **L4** with one intact C−H bond was treated with the [(Cp*Ir)$_2$(pyrazine)] fragment under the same conditions (Scheme 3). After purification, a red crystalline solid consisting of [(Cp*Ir)(*o*-O$_2$C−C$_2$B$_{10}$H$_{10}$)]$_2$(pyrazine) **6** was isolated. Subsequently, it is a natural extension for us to examine the reactivity of monosubstituted *p*-carborane carboxylate. However, this ligand was not obtained due to difficulties in the purification process. Therefore, another *p*-carborane monocarboxylic acid ligand **L5** was treated with **2**, affording B−H activation and binuclear iridium complex [(Cp*Ir)$_2$[*p*-O$_2$C−C$_2$B$_{10}$H$_9$−(C(OH)^{n}Bu$_2$)]$_2$pyrazine] **7** (Scheme 3), which suggests that a directing group in the ligand is important. The ^{1}H NMR spectrum of **7** showed three signals at δ 0.91, 1.42, and 1.87 ppm, which were attributed to the ^{n}Bu group of the carborane ligand. The characteristic signals of the pyrazine and Cp* groups in complex **7** are at δ 8.57 and 1.28 ppm, respectively, which are similar to those of **5**.

The cage C−H activation of carborane to form **6** was first observed directly from its X-ray crystal structure (Figure 5). Such reactivity, which is analogous to that of substituted phenyl rings, further reveals the "*pseudoaromatic*" property of the carborane cage and shows that this icosahedron cage can serve

Scheme 3. Synthesis of Binuclear Complexes 6 and 7

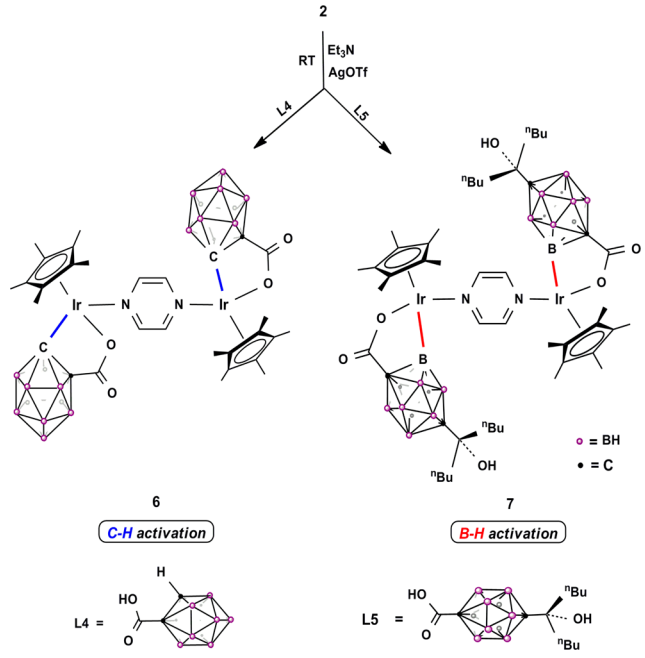

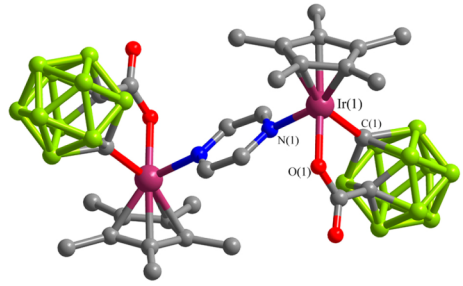

6

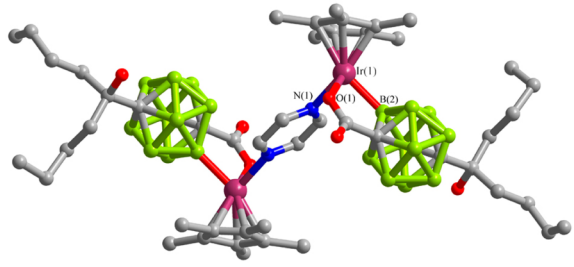

7

Figure 5. X-ray crystal structures of complexes **6** and **7**. H atoms and solvent molecules are omitted for clarity. Plum, Ir; Gray, C; Red, O; Blue, N; Lime, B. Selected bond lengths (Å) and angles (deg): **6**, Ir(1)−C(1), 2.116(8); Ir(1)−O(1), 2.151(5). **7**, Ir(1)−B(2), 2.115(9); Ir(1)−O(1), 2.128(6); O(1)−Ir(1)−B(2), 79.6(3).

as a "three-dimensional benzene". The coordination sets of the Cp*Ir centers are occupied by the pyrazine N atoms, and the O and C atoms of two mono-*o*-carborane carboxylates. The Ir−C bond length of **6** is 2.116(8) Å, which is very similar to those of our previous reports.[14]

For the reaction between **2** and the smaller monocarboxylic acid ligand **L$_4$**, the calculations are less expensive and can be studied in more detail. Initially, **L$_4$** can also form a stable

dx.doi.org/10.1021/ja4115665 | J. Am. Chem. Soc. 2014, 136, 2825−2832

bidentate complex (**bd-2-L$_4$**$^{2+}$) with **2**$^{4+}$ after the proton of the carboxyl group is removed by Et_3N. In order to adopt a favorable conformation for the subsequent deprotonation process, **bd-2-L$_4$**$^{3+}$ also needs to convert to a monodentate conformation **md-2-L$_4$**$^{3+}$. After losing a proton from C−H or B−H, the deprotonated product **md-2-L$_4$**$^{2+}$ then converts to the final C−H activation product **6**$^{2+}$(**C**$^-$), or the B−H activation product **6**$^{2+}$(**B**$^-$). Although the direct insertion of metal center into B−H bonds has been reported in the literature[18,19] due to its σ-donor ability,[20] for the reaction of **2** with **L$_1$**, our calculations showed that the insertion product of Ir into the B−H bond is more unstable than the initial bidentate conformation **bd-2-L$_1$**$^{2+}$ by 63.9 kcal/mol, making this direct insertion route very unlikely. This is probably due to the bulky pyrazine ligand in **2** which makes such an insertion product very crowded around the Ir center. In contrast, in literature examples, the ligands around Ir are less sterically crowding since there are two hydrogens on Ir.[18a] Therefore, for the reaction between **2** and **L$_4$** we studied the deprotonation of **md-2-L$_4$**$^{3+}$ by Et_3N. The resulting Gibbs free energy profiles are presented in Figure 6 (top), while the optimized geometries of the intermediates and transition states are presented in the bottom of Figure 6. It can be seen that the overall Gibbs free energy barrier $\Delta G^{\ddagger}$ of the C−H activation pathway is just 27.0 kcal/mol. On the other hand, $\Delta G^{\ddagger}$ of the B−H activation pathway is 41.1 kcal/mol. Therefore, C−H of **L$_4$** is much more likely to be activated than B−H. This is due to the stronger acidity of C−H over that of B−H groups and also that the resulting C$^-$ is more stable than B$^-$ (as shown in Figure 6) by 7.6 kcal/mol in free energy. This is in good agreement with experiment, in which no B−H activation products were observed in the reaction between **2** and **L$_4$**.

It is concluded that C−H activation takes place preferentially to B−H activation under the same mild conditions from both experimental and theoretical studies, which means that the sp^2 B−H bond is more stable than the sp^2 C−H bond. The results also suggest that selective bond functionalization can be obtained through versatile ligand design. On the other hand, it is significant that C−H activation mediated by transition metal complexes has been widely exploited because of its potential utilization in both pharmaceutical industrial applications that produce different types of heterocycles.[17] Especially C−H activation of carborane derivatives has presumably contributed to the belated arrival of "borametallic" chemistry.[21]

The molecular structure of **7** consists of two Cp*Ir fragments connected by a pyrazine molecules through N atoms and coordinated by carborane ligands through one O atom and one B atom (at the B(2) position) to form *Z*-shape architecture (Figure 5). The Ir−N (pyrazine), Ir−O (carboxyl), and Ir−B(2) bond distances in complex **7** (2.081(6), 2.128(6) and 2.115(9) Å) are similar to those of complex **5**. The N(pyrazine)−Ir−B(2) angle in **7** is different from that of **5** with a right angle 89.59(3)° compared to 91.2(9)°, which is favorable for forming a zigzag backbone.

3. CONCLUSIONS

In summary, a facile and efficient route to carborane-based metallacycles has been developed by exploiting metal-induced B−H activation. Using the directional bonding approach (Ir−B coordination), two Ir-based metallacycles and one binuclear complex were synthesized through regioselective B−H activation under mild conditions, in contrast to a the previous report describing the self-assembly of coordination-driven

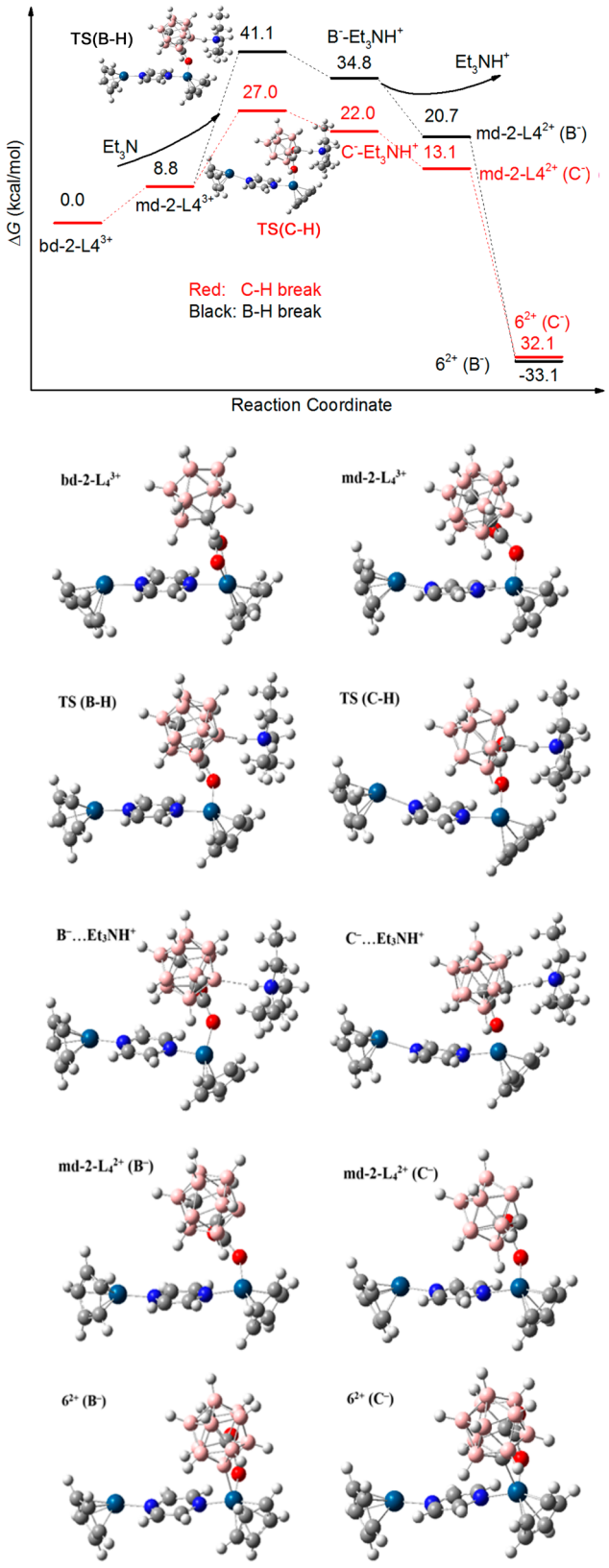

Figure 6. Gibbs free energy profiles (in kcal/mol, at 298 K) of the reaction between **2**$^{4+}$ and **L$_4$**$^{1-}$ where the red line represents the C−H activation pathway and the black line represents the B−H activation pathway (top). Geometries of the intermediates and transition states in the reaction between **2**$^{4+}$ and **L$_4$**$^{1-}$ (bottom).

dx.doi.org/10.1021/ja4115665 | *J. Am. Chem. Soc.* 2014, 136, 2825−2832

metallamacrocycles with a carborane backbone acting as a simple bridging ligand. Additionally, experimental results and DFT calculations both indicate that cage C_c−H bond activation preferentially takes place over B−H activation under the same conditions. These results may suggest that the iridium-mediated functionalization of carboranes through insertion of unsaturated molecules into Ir−C(B) bonds to form C−C(B) bonds is practical, and further application in this field is the target of continued efforts.

4. EXPERIMENTAL SECTION

To a solution of $[Cp^*IrCl(\mu\text{-}Cl)]_2$ (80 mg, 0.1 mmol) in CH_2Cl_2 (20 mL) was added pyrazine (8 mg, 0.1 mmol) at room temperature. After vigorous stirring for 4 h, AgOTf (102 mg, 0.4 mmol) was then added to the solution, and the reaction was carried out in the dark. Finally, L1 (23.4 mg, 0.1 mmol)/L2 (23.4 mg, 0.1 mmol)/L3 (23.4 mg, 0.1 mmol)/L4 (38.0 mg, 0.2 mmol)/L5 (64.0 mg, 0.2 mmol) was added to the solution with Et_3N (0.5 mL), and vigorous stirring was continued for 12 h. Then the solution was filtered to remove undissolved solid. The filtrate was concentrated and further purified via neutral alumina gel chromatography (CH_2Cl_2, CH_3OH).

■ ASSOCIATED CONTENT

Supporting Information

Experimental details, characterization data, ^1H and ^{11}B NMR spectra, DFT computational details and crystallographic data (CIF) for **3**−**7**. This material is available free of charge via the Internet at http://pubs.acs.org.

■ AUTHOR INFORMATION

Corresponding Author

gxjin@fudan.edu.cn

Notes

The authors declare no competing financial interest.

■ ACKNOWLEDGMENTS

This work was supported by the National Science Foundation of China (91122017, 21374019, 21273042), the Shanghai Science and Technology Committee (13JC1400600, 13DZ2275200), and the Program for Changjiang Scholars and Innovative Research Team in University (IRT1117).

■ REFERENCES

(1) (a) Irvine, G. J.; Lesley, M. J. G.; Marder, T. B.; Norman, N. C.; Rice, C. R.; Robins, E. G.; Roper, W. R.; Whittell, G. R.; Wright, L. J. *Chem. Rev.* **1998**, *98*, 2685. (b) Braunschweig, H. *Angew. Chem., Int. Ed.* **1998**, *37*, 1786.

(2) (a) Beletskaya, I.; Pelter, A. *Tetrahedron* **1997**, *53*, 4957. (b) Smith, M. R., III. *Prog. Organomet. Chem.* **1999**, *48*, 505.

(3) Mckay, D.; Macgregor, S. A.; Rosair, G. M.; Welch, A. J. *Angew. Chem., Int. Ed.* **2010**, *49*, 4943.

(4) (a) Chen, H.; Schlecht, S.; Semple, T. C.; Hartwig, J. F. *Science* **2000**, *287*, 1995. (b) Kawamura, K.; Hartwig, J. F. *J. Am. Chem. Soc.* **2009**, *131*, 9201.

(5) (a) Miyaura, N. In *Catalytic Heterofunctionalization*; Togni, A.; Grützmacher, H., Eds.; Wiley-VCH: Weinheim, 2001; pp 1−45. (b) Hartwig, J. F.; Cook, K. S.; Hapke, M.; Incarvito, C. D.; Fan, Y.; Webster, C. E.; Hall, M. B. *J. Am. Chem. Soc.* **2005**, *127*, 2538. (c) Mkhalid, I. A. I.; Barnard, J. H.; Marder, T. B.; Murphy, J. M.; Hartwig, J. F. *Chem. Rev.* **2010**, *110*, 890. (d) Segawa, Y.; Yamashita, M.; Nozaki, K. *J. Am. Chem. Soc.* **2001**, *123*, 8422.

(6) (a) Hawthorne, M. F.; Zheng, Z.-P. *Acc. Chem. Res.* **1997**, *30*, 267. (b) Valliant, J. F.; Guenther, K. J.; King, A. S.; Morel, P.; Schaffer, P.; Sogbein, O. O.; Stephensen, K. *Coord. Chem. Rev.* **2002**, *232*, 173. (c) Liu, S.; Han, Y.-F.; Jin, G.-X. *Chem. Soc. Rev.* **2007**, *36*, 1543. (d) Chizhevsky, I. T. *Coord. Chem. Rev.* **2007**, *251*, 1590. (e) Xie, Z. *Acc. Chem. Res.* **2003**, *36*, 1. (f) Bregadze, V. I. *Chem. Rev.* **1992**, *92*, 209. (g) Plešek, J. *Chem. Rev.* **1992**, *92*, 269. (h) Scholz, M.; Hey-Hawkins, E. *Chem. Rev.* **2011**, *111*, 7035. (i) Yao, Z.-J.; Jin, G.-X. *Coord. Chem. Rev.* **2013**, *257*, 2522.

(7) (a) Bae, J.-Y.; Lee, Y.-J.; Kim, S.-J.; Ko, J.; Cho, S.; Kang, S. O. *Organometallics* **2000**, *19*, 1514. (b) Yao, Z.-J.; Su, G.; Jin, G.-X. *Chem.—Eur. J.* **2011**, *17*, 13298. (c) Yao, Z.-J.; Jin, G.-X. *Organometallics* **2011**, *30*, 5365.

(8) (a) Stang, P. J.; Olenyuk, B. *Acc. Chem. Res.* **1997**, *30*, 502. (b) Seidel, S. R.; Stang, P. J. *Acc. Chem. Res.* **2002**, *35*, 972. (c) Gianneschi, N. C.; Masar, M. S.; Mirkin, C. A. *Acc. Chem. Res.* **2005**, *38*, 825. (d) Fujita, M. *Chem. Soc. Rev.* **1998**, *27*, 417. (e) Fujita, M.; Tominaga, M.; Hori, A.; Therrien, B. *Acc. Chem. Res.* **2005**, *38*, 369. (f) Cotton, F. A.; Lin, C.; Murillo, C. A. *Acc. Chem. Res.* **2001**, *34*, 759. (g) Caulder, D. L.; Raymond, K. N. *Acc. Chem. Res.* **1999**, *32*, 975. (h) Chakrabarty, R.; Mukherjee, P. S.; Stang, P. J. *Chem. Rev.* **2011**, *111*, 6810. (i) Wiester, M. J.; Ulmann, P. A.; Mirkin, C. A. *Angew. Chem., Int. Ed.* **2011**, *50*, 114. (j) Severin, K. *Chem. Commun.* **2006**, 3859.

(9) (a) Vajpayee, V.; Song, Y. H.; Cook, T. R.; Kim, H.; Lee, Y.; Stang, P. J.; Chi, K.-W. *J. Am. Chem. Soc.* **2011**, *133*, 19646. (b) Zheng, Y.-R.; Lan, W.-J.; Wang, M.; Cook, T. R.; Stang, P. J. *J. Am. Chem. Soc.* **2011**, *133*, 17045. (c) Pollock, B. J.; Cook, T. R.; Stang, P. J. *J. Am. Chem. Soc.* **2012**, *134*, 10607. (d) Pollock, B. J.; Schneider, G. L.; Cook, T. R.; Davies, A. S.; Stang, P. J. *J. Am. Chem. Soc.* **2013**, *135*, 13676. (e) Zheng, Y.-R.; Yang, H.-B.; Northrop, B. H.; Ghosh, K.; Stang, P. J. *Inorg. Chem.* **2008**, *47*, 4706. (f) Yang, H.-B.; Das, N.; Huang, F.; Hawkridge, A. M.; Muddiman, D. C.; Stang, P. J. *J. Am. Chem. Soc.* **2006**, *128*, 10014.

(10) (a) Fujita, D.; Takahashi, A.; Sato, S.; Fujita, M. *J. Am. Chem. Soc.* **2011**, *133*, 13317. (b) Yoneya, M.; Yamaguchi, T.; Sato, S.; Fujita, M. *J. Am. Chem. Soc.* **2012**, *134*, 14401. (c) Fang, Y.; Murase, T.; Sato, S.; Fujita, M. *J. Am. Chem. Soc.* **2013**, *135*, 613. (d) Yoshizawa, M.; Klosterman, J. K.; Fujita, M. *Angew. Chem., Int. Ed.* **2009**, *48*, 3418.

(11) (a) Caulder, D. L.; Powers, R. E.; Parac, T. N.; Raymond, K. N. *Angew. Chem., Int. Ed.* **1998**, *37*, 1840. (b) Brown, C. J.; Miller, G. M.; Johnson, M. W.; Bergman, R. G.; Raymond, K. N. *J. Am. Chem. Soc.* **2011**, *133*, 11964. (c) Hart-Cooper, W. M.; Clary, K. N.; Toste, F. D.; Bergman, R. G.; Raymond, K. N. *J. Am. Chem. Soc.* **2012**, *134*, 17873.

(12) Smulders, M. M. J.; Zarra, S.; Nitschke, J. R. *J. Am. Chem. Soc.* **2013**, *135*, 7039. (b) lliger, J. L.; Belenguer, A. M.; Nitschke, J. R. *Angew. Chem., Int. Ed.* **2013**, *52*, 7958. (c) Granzhan, A.; Schouwey, C.; Riis-Johannessen, T.; Scopelliti, R.; Severin, K. *J. Am. Chem. Soc.* **2011**, *133*, 7106. (d) Schmitt, F.; Freudenreich, J.; Barry, N. P. E.; Juillerat-Jeanneret, L.; Süss-Fink, G.; Therrien, B. *J. Am. Chem. Soc.* **2012**, *134*, 754. (f) Huang, S.-L.; Lin, Y.-J.; Hor, T. S. A.; Jin, G.-X. *J. Am. Chem. Soc.* **2013**, *135*, 8125.

(13) (a) Wedge, T. J.; Hawthorne, M. F. *Coord. Chem. Rev.* **2003**, *240*, 111. (b) Clegg, W.; Gill, W. R.; MacBride, J. A. H.; Wade, K. *Angew. Chem., Int. Ed.* **1993**, *32*, 1328. (c) Jude, H.; Disteldorf, H.; Fischer, S.; Wedge, T.; Hawkridge, A. M.; Arif, A. M.; Hawthorne, M. F.; Muddiman, D. C.; Stang, P. J. *J. Am. Chem. Soc.* **2005**, *127*, 12131. (d) El-Kaderi, H. M.; Hunt, J. R.; Mendoza-Cortés, J. L.; Côté, A. P.; Tylor, R. E.; O'Keeffe, M.; Yaghi, O. M. *Science* **2007**, *316*, 268.

(14) (a) Yu, W.-B.; Han, Y.-F.; Lin, Y.-J.; Jin, G.-X. *Organometallics* **2010**, *29*, 2827. (b) Yu, W.-B.; Han, Y.-F.; Lin, Y.-J.; Jin, G.-X. *Chem.—Eur. J.* **2011**, *17*, 1863.

(15) (a) Jin, G.-X.; Wang, J.-Q.; Zhang, C.; Weng, L.-H.; Herberhold, M. *Angew. Chem., Int. Ed.* **2005**, *44*, 259. (b) Yao, Z.-J.; Xu, B.; Jin, G.-X. *J. Organomet. Chem.* **2012**, *721*−*722*, 31.

(16) (a) Spokoyny, A. M.; Reuter, M. G.; Stern, C. L.; Ratner, M. A.; Seideman, T.; Mirkin, C. A. *J. Am. Chem. Soc.* **2009**, *131*, 9482. (b) El-Zaria, M. E.; Arii, H.; Nakamura, H. *Inorg. Chem.* **2011**, *50*, 4149.

(17) (a) Ryabov, A. D. *Chem. Rev.* **1990**, *90*, 403. (b) Arndtsen, B. A.; Bergman, R. G.; Mobely, T. A.; Peterson, T. H. *Acc. Chem. Res.* **1995**, *28*, 154. (c) Ritleng, V.; Sirlin, C.; Preffer, M. *Chem. Rev.* **2002**, *102*, 1731. (d) Zeni, G.; Larock, R. C. *Chem. Rev.* **2004**, *104*, 3341.

(e) Chiou, W. H.; Lee, S. Y.; Ojima, I. *Can. J. Chem.* **2005**, *83*, 681. (f) Zeni, G.; Larock, R. C. *Chem. Rev.* **2006**, *106*, 4644.
(18) (a) Lee, Y.-J.; Lee, J.-D.; Kim, S.-J.; Ko, J.; Suh, I.-H.; Cheong, M.; Kang, S. O. *Organometallics* **2004**, *23*, 135. (b) Hoel, E. L.; Hawthorne, M. F. *J. Am. Chem. Soc.* **1973**, *95*, 2712.
(19) Segawa, Y.; Yamashita, M.; Nozaki, K. *J. Am. Chem. Soc.* **2009**, *131*, 9201.
(20) (a) Zhu, J.; Lin, Z. Y.; Marder, T. B. *Inorg. Chem.* **2005**, *44*, 9384. (b) Segawa, Y.; Yamashita, M.; Nozaki, K. *Angew. Chem., Int. Ed.* **2007**, *46*, 6710. (c) Braunschweig, H.; Brenner, P.; Müller, A.; Radacki, K.; Rais, D.; Uttinger, K. *Chem.—Eur. J.* **2007**, *13*, 7171. (d) Braunschweig, H.; Radacki, K.; Uttinger, K. *Chem.—Eur. J.* **2008**, *14*, 785. (e) Braunschweig, H.; Green, H.; Radacki, K.; Uttinger, K. *Dalton Trans.* **2008**, 3531. (f) Dang, L.; Zhao, H.; Lin, Z.; Marder, T. B. *Organometallics* **2008**, *27*, 1178. (g) Braunschweig, H.; Leech, R.; Rais, D.; Radacki, K.; Uttinger, K. *Organometallics* **2008**, *27*, 418.
(21) Braunschweig, H.; Dewhurst, R. D.; Schneider, A. *Chem. Rev.* **2010**, *110*, 3924.